Journal of Communications Technology and Electronics, Vol. 48, No. 1, 2003, pp. 105–113. Translated from Radiotekhnika i Elektronika, Vol. 48, No. 1, 2003, pp. 116–124.

MICROWAVE ELECTRONICS

Synchronization of a Chaotic Self-Oscillations in the "Spiral Electronic Beam—Counterpropagating Electromagnetic Wave" Distributed System

D. I. Trubetskov and A. E. Khramov

Received April 12, 2002

Abstract—The influence of an external harmonic signal on a chaotic generation in the distributed active medium of a spiral electron beam interacting with a counterpropagating waveguide wave (the cyclotron-resonance maser with a counterpropagating traveling wave) is investigated for the first time. The characteristics of nonautonomous space-time oscillations are studied. The physical processes accompanying the transition of a distributed self-oscillating system with complicated space-time dynamics to the synchronization mode are considered.

INTRODUCTION

The studies of the synchronization of nonlinear systems demonstrating deterministic chaos have recently been attracting more and more interest (see, e.g., works [1–3]). A large number of publications (see references in reviews [1–3]) deal with chaos synchronization in discrete (mappings) and streaming finite-dimensional systems. According to these works, various types of synchronization of chaotic systems can be considered. The strictest definition of synchronization requires that the difference in the state vectors of the system under study and the external action (for example, from another chaotic system coupled with the first one) tend to zero at $t \longrightarrow \infty$. This is the so-called *identical* synchronization, which is rarely used in practice. More often, the term *generalized* synchronization is used [1], which implies that the system's state should asymptotically tend to some function (possibly a rather complicated one). Generalized synchronization also includes the classical definition of synchronization in self-oscillating systems, such as the Van der Pol oscillator [4].

When analyzing the synchronization of chaotic systems, it is convenient to use the term *phase* synchronization of chaotic oscillations, first introduced by Rosenblum [5]. In this case, to analyze the synchronization of the system under study, the phase of chaotic oscillations $\phi(t)$ should be introduced. The phase of a chaotic signal is introduced strictly using the Gilbert transformation [5, 6], however, in the case of a complicated chaotic signal, good results can hardly be obtained. Therefore, the phase $\phi(t)$ is more often introduced phenomenologically, being defined by the analysis of the basic characteristic scale of oscillations of the chaotic system. For example, if a chaotic attractor has a belt or a spiral form in the phase space, one can introduce a characteristic return time of the attractor phase trajectory to the selected plane. At the instant of return, the phase of the chaotic signal can be changed by 2π. One can assume that phase of the phase trajectory changes linearly between two intersections of a selected plane. Various ways of introducing the signal's phase $\phi(t)$ for finite-dimensional systems are described in [7, 8]. If the phase $\phi(t)$ is defined, one can introduce the characteristic frequency $\bar{\omega}$ of the chaotic signal as

$$\bar{\omega} = \lim_{t \to \infty} \phi(t)/t. \quad (1)$$

When a chaotic system is affected by an external harmonic signal with frequency Ω, the phase synchronization takes place when $\bar{\omega} = \Omega$. In this case, the characteristic base frequency of chaotic self-oscillations of the system equals the frequency of external influence, i.e., a locking of oscillations by the control signal takes place, as in the case of periodic oscillations. It is important that, at the phase synchronization, the time dependence of the signal amplitude can be rather complicated, manifesting chaotic behavior, but the characteristic time scale of oscillations will be determined by the control signal.

Note that all the results concerning synchronization of chaotic self-oscillations dealt with investigations of the dynamics of finite-dimensional systems. We are not aware of any works analyzing the synchronization of chaotic oscillation modes in the distributed active media. However, it is the distributed systems that cause a special interest for both the fundamental study on the control of the complex dynamics and chaos in the dynamic systems of various nature and for the practical application of results.

The problem of synchronization of chaotic self-oscillations in the relativistic vacuum microwave electronic systems is particularly important. On the one hand, this problem applies to the construction of superpowered microwave generators with tunable characteristics (frequency, bandwidth, power level) of output radiation. On the other hand, the study of the effect of

external signals is important for designing the microwave generators used as modules in the phase array antennas controlled by external signals.

The present work studies the influence of an external harmonic signal on the chaotic generation in the "spiral electronic beam—counterpropagating electromagnetic wave" system (cyclotron-resonance maser (CRM) with a counterpropagating traveling wave). A characteristic feature of the counterpropagating-wave CRM is the possibility of effective tuning of the oscillation frequency by changing either the longitudinal velocity $v_\parallel$ of electrons, or the static magnetic field B_0. For this purpose, a real device would require changing both the geometry of the guiding structure and the magnitude of the magnetic field along the interaction space [9], which would naturally complicate the theory. Therefore, the mathematical model developed below is an idealized one in this sense.

In Section 1, we formulate the mathematical model used to investigate the nonautonomous operating mode of the CRM with a counterpropagating wave. In Section 2, the modes of nonautonomous oscillations in the system are briefly discussed, and Section 3 deals with characteristics of the synchronization mode. In Section 4, the physical processes in the system under study are discussed.

1. MATHEMATICAL MODEL

The interaction of a weakly relativistic cylindrical helical beam with a counterpropagating wave is described by the following self-consistent system of equations for the weakly relativistic electron beam [10] and the counterpropagating wave excited by the electron flow [10–12]:

$$\frac{d\beta}{d\xi} - j\mu(1-|\beta|^2)\beta = F, \tag{2}$$

$$\frac{\partial F}{\partial \tau} - \frac{\partial F}{\partial \xi} = -I, \quad I = \frac{1}{2\pi}\int_0^{2\pi} \beta d\theta_0, \tag{3}$$

where $\beta = r\exp(j\theta)$ is the complex radius of trajectories of the electron ensemble with the uniform initial phase distribution with respect to the high-frequency (HF) field, $F = F(\xi, \tau)$ is the slowly varying dimensionless complex field amplitude in the beam cross-section, $I = I(\xi, \tau)$ is the first harmonic of the bunched current, $\xi = \beta_0(\hat\omega)\varepsilon z$ is the dimensionless longitudinal coordinate, $\tau = \hat\omega\varepsilon(t - z/v_\parallel)(1 + v_\parallel/|v_g|)^{-1}$ is the dimensionless time in the coordinate frame which moves with the beam's longitudinal velocity $v_\parallel$, and $\hat\omega$ is the frequency over which the averages are taken. Frequency $\hat\omega$ satisfies the synchronism condition

$$\hat\omega + \beta_0(\hat\omega)v_\parallel - \omega_c = 0. \tag{4}$$

Here $\beta_0(\hat\omega)$ is the propagation constant of the counterpropagating wave with frequency $\hat\omega$ in the system without the electron beam and v_g is the group velocity of the wave at frequency $\hat\omega$. We also introduced the nonisochronism parameter

$$\mu = (v_\parallel/c)/2\varepsilon,$$

characterizing the inertiality of the system, interaction parameter

$$\varepsilon = \left(\frac{I_0 K}{4V_0}\left(1 + \frac{v_{\perp 0}^2}{v_\parallel^2}\right)\right)^{0.5} \ll 1,$$

and cyclotron frequency at $\xi = 0$

$$\omega_c = \frac{eB_0}{m_0 c}\left(1 - \frac{1}{2}\frac{v_\parallel^2 + v_{\perp 0}^2}{c^2}\right);$$

K is the coupling resistance, $v_{\perp 0}$ is the initial transverse velocity of electrons, and I_0 and V_0 are the dc components of the current and voltage of the beam.

Equations (2)–(3) are solved with the following initial and boundary conditions:

$$F(\xi, \tau = 0) = f^0(\xi), \quad \beta(\xi = 0) = \exp(j\theta_0), \quad \theta_0 \in [0, 2\pi]. \tag{5}$$

The external harmonic control signal $F(\xi = A, \tau) = F_0 e^{j\Omega\tau}$ is applies at the collector end $\xi = A$ of the system. Here, A is the system's length, F_0 is the amplitude of external signal, and Ω is the detuning of the external influence from the frequency $\hat\omega$ of the "cold" synchronism (see condition (4)).

The model described by Eqs. (2)–(5) is valid under the following conditions: the field in the cross section of the electron beam should be uniform; the longitudinal velocity $v_\parallel \approx$ const (i.e., the interaction of oscillating electrons with the HF components of the magnetic field is neglected); and the nonstationary process is supposed to be the narrowband one, so that, in the operating frequency range, the helical beam is supposed to interact only with the counterpropagating wave.

Works [13, 14] investigate the dynamics of the system considered in the autonomous mode and show the presence of various modes of space-time oscillations. At a specified value of nonisochronism parameter $\mu > 2$, the modes successively change from stationary generation through periodic to chaotic self-modulation with increasing system length A.

2. DYNAMICS OF A NONAUTONOMOUS SYSTEM

Figure 1 demonstrates the mode map on the plane of control parameters (amplitude F_0 and frequency Ω of the nonautonomous generator with a helical beam). Figure 2 demonstrates the power spectra $P(f)$ of the

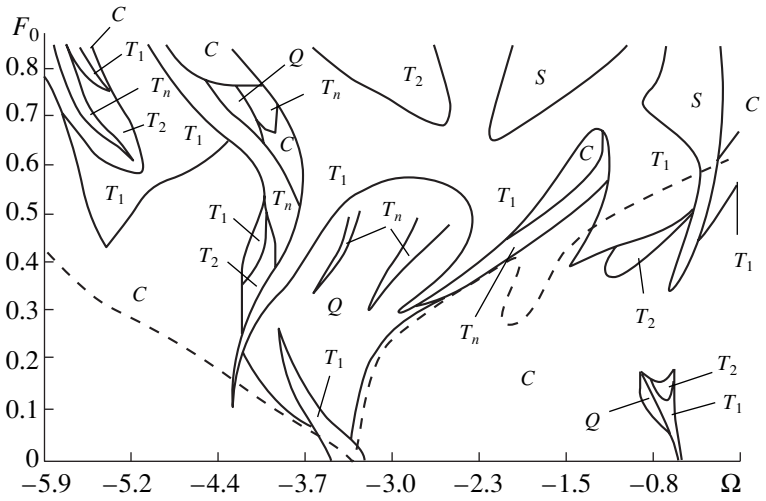

Fig. 1. Plane of control parameters (Ω and amplitude F_0) with characteristic modes of nonautonomous oscillations in a CRM with counterpropagating wave. Dashed line indicates the quasi-synchronization region.

output field (left column) and time dependences of the slowly varying field amplitude $|F(\xi = 0, \tau)|$ (right column). It should be noted that the stationary generation mode of the CRM corresponds to the power spectrum with a single base frequency $f_0 = \omega_0/2\pi$ (see Fig. 2). Actually, the $|F|$ curve is the envelope of the HF signal, whose spectrum is presented nearby. Let us briefly consider the generation modes emerging in a nonautonomous system by analyzing Figs. 1 and 2.

Figure 2a demonstrates the characteristics of the autonomous chaotic oscillations in a CRM with a counterpropagating wave at the nonisochronism parameter $\mu = 8.0$ and the system length $A = 3.0$. The generated spectrum clearly manifests the base spectral component $f_0 = -0.51$ against the developed noise pedestal of about 30–40 dB.

The modes of nonautonomous generation are marked by different symbols on the mode map (see Fig. 1): *C* is the chaotic self-modulation of the output signal $F(\xi = 0, \tau)$; *Q* is the quasi-periodic self-modulation, i.e., the self-modulation with two incommensurable spectral components; T_1 are the modes of periodic self-modulation of the output signal; T_2 are the modes of the period-doubling self-modulation; T_n are the modes of the complex-period self-modulation; and *S* are the modes of stationary generation.

At small amplitudes of external influence F_0 and considerable detuning of the external frequency from that of autonomous oscillations $|\Omega - \omega_{0A}|$, chaotic oscillations of the output signal amplitude occur (see Fig. 1, region *C*). The characteristics of the oscillations in the mode characterized by the chaotic self-modulation of the output signal $|F(\tau)|$ are presented in Fig. 2b for the external signal parameters $F_0 = 0.22$ and $\Omega = -4.48$. One can see that, in this case, characteristics of the chaotic oscillations of the output field are similar to those of the autonomous oscillation mode. The characteristic amplitude of the self-modulation of the output signal, which can be estimated from the time realization $|F(\tau)|$ (Fig. 2b, right) in the nonautonomous self-oscillation mode, is strongly dependent on the parameters of the control signal.

At $\Omega \sim \omega_{0A}$ and $F_0 < 0.5$, a quasi-periodic self-modulation of the output signal with frequencies f_1 and f_2 is observed (see Fig. 1, region *Q*, and curves in Fig. 2c plotted at $F_0 = 0.22$ and $\Omega = -3.48$). The output signal spectrum contains three incommensurable base frequency components f_0, f_1, and f_2 (Fig. 2c).

At greater amplitudes of external influence ($F_0 > 0.4$), the modes change with the parameters of the control signal in a rather complicated way: there is a large number of order-to-chaos and chaos-to-order transitions. At $\Omega \sim \omega_{0A}$, a region of periodic self-modulation of the output signal is observed (region T_1 in Fig. 1). In this case, the oscillation characteristics are presented in Fig. 2d ($F_0 = 0.62$ and $\Omega = -3.48$). The output signal spectrum contains two base frequencies f_0 (the frequency of HF generation) and f_1 (the self-modulation frequency) (Fig. 2d); i.e., the output oscillations are quasi-periodic and are represented in the phase space by a torus.

One can see from Fig. 1 that, at increasing amplitudes of external influence, the modes of the complex-period self-modulation (regions T_2 and T_n) and the stationary generation (region *S*) are observed in the presence of the latter mode. The corresponding oscillation characteristics are demonstrated in Fig. 2e. One can see that the output signal amplitude $|F(\tau)|$ becomes constant $|F(\tau)| = \text{const}$ after a long transient process. The power spectrum of the output signal contains only one spectral component corresponding to the frequency f_0 of HF generation.

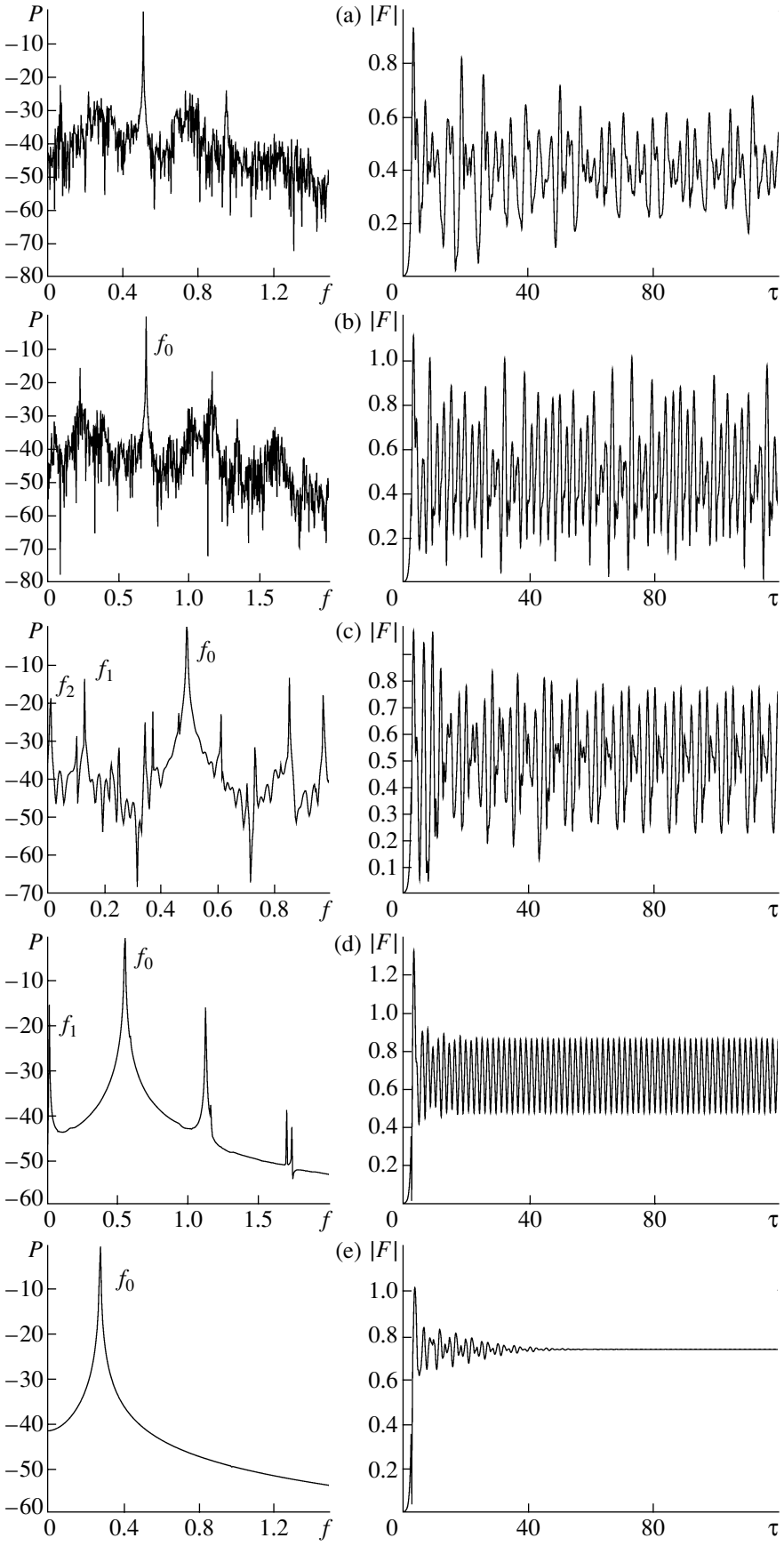

Fig. 2. Oscillation characteristics in various generation modes.

3. SYNCHRONIZATION MODE

Let us consider the synchronization mode in the active distributed oscillating system under study. By the term "phase synchronization of chaos" (see Introduction), we mean locking of the HF generation frequency ω_0 by an external control signal. The frequency of HF generation is determined as a correction ω_0 to the frequency $\hat{\omega}$ of the "cold" synchronism. Frequency ω_0 is determined by phase $\varphi_F(\xi, \tau)$ of the field $F(\xi, \tau) = |F(\xi, \tau)|\exp\{j\varphi_F(\xi, \tau)\}$. In the case of the single-frequency HF generation, the correction to the output signal frequency can be written as

$$\omega_0 = \lim_{t \to \infty} \varphi_F(\xi = 0, \tau)/t. \quad (6)$$

If phase $\varphi_F(\xi, \tau)$ is assumed to be a periodic function with period 2π, i.e., the function

$$\bar{\varphi}_F(\xi, \tau) = \varphi_F(\xi, \tau) \mod 2\pi$$

is considered, then $\bar{\varphi}_F$ is a periodic function with the period $1/\omega_0$. In the case of the complex dynamics of phase $\bar{\varphi}_F(\tau)$, frequency ω_0 (which can be found from relationship (6)) determines the main characteristic time scale of the HF generation in the helical beam.

The phase synchronization mode (further called the quasi-synchronization mode) is characterized by the condition $\omega_0 = \Omega$. In this case, the amplitude of the output HF field $|F(\tau)|$ can vary in time in a rather complicated way, demonstrating both the periodic and chaotic self-modulation modes.

In Fig. 1, the dashed line shows the area of quasi-synchronization of the counterpropagating-wave CRM by the external control signal. In this area, the amplitude self-modulation of the output signal is observed, which can be clearly seen from the mode map. However, the HF generation frequency ω_0 (see Fig. 2b corresponding to the quasi-synchronization mode, frequency $f_0 = \omega_0/2\pi$ is marked on the figure) of the system is determined by frequency Ω of the control signal, so that $\omega_0 = \Omega$.

Figure 3 demonstrates the frequency difference $(\Omega - \omega)$ of HF output oscillations versus frequency Ω at various amplitudes F_0 of the control signal. In the area of quasi-synchronization, the difference $\Omega - \omega = \text{const}$. In the outer regions, with detuning off the boundary of the synchronization area, the generation frequency tends to the frequency of autonomous generation (see Fig. 3a).

The width of the quasi-synchronization area increases with the amplitude of external influence, and, at the negative detuning $(\Omega - \omega) < 0$, the width of the synchronization "beak" is actually a linear function of frequency Ω. The right boundary of the quasi-synchronization area has a more complex shape.

At greater values of external signal amplitude ($0.25 < F_0 < 0.45$), one more synchronization beak

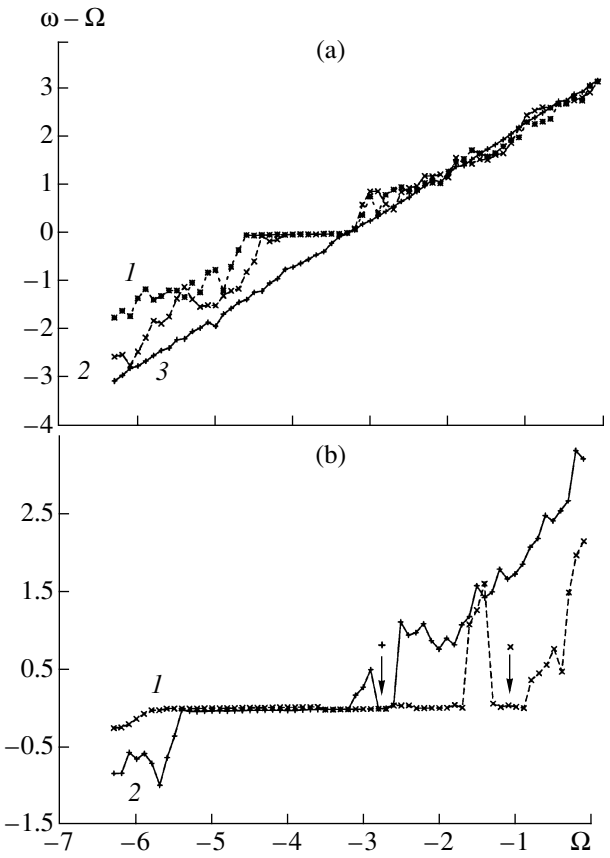

Fig. 3. Frequency difference $\Omega - \omega$ at the system output as a function of frequency Ω at various amplitudes F_0 of the control signal: (a) F_0 = (*1*) 0.22, (*2*) 0.12, and (*3*) 0.02; (b) F_0 = (*1*) 0.42 and (*2*) 0.32.

appears at the frequencies of external influence $\Omega \in (-2.0, -1.5)$ (see Fig. 3b, curves *1* and *2*). One can see that, with changing frequency Ω, two areas of different width exist where the oscillation frequency is locked by the external signal. The arrow indicates the regions of the curve corresponding to the second area of synchronization. The width of the second synchronization beak increases with the amplitude of external influence until it merges with the main beak.

Note that a similar picture was observed [15] in the analysis of the synchronization of two coupled oscillators with virtual cathode operating in a strongly nonlinear mode. It was shown [15] that, varying the beam current of each generator (which corresponds to the frequency tuning of the autonomous oscillation in each module), one can observe a synchronization area of a complex shape. This are a contains two subregions corresponding to different frequencies of autonomous oscillations of the generators.

4. PHYSICAL PROCESSES

Let us consider the physical processes in a helical electron beam interacting with a counterpropagating

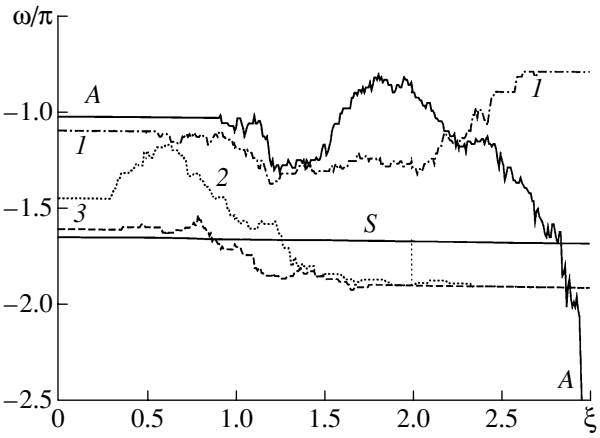

Fig. 4. Characteristic frequency of self-oscillations in various cross-sections of the interaction space for different characteristic modes of the system. Curve *A* corresponds to the autonomous space-time oscillations; curve *S*, to quasi-synchronization mode ($\Omega = -5.3$, $F_0 = 0.42$, when the periodic self-modulation of the output signal is observed); and curves *1–3*, to the chaotic self-modulation modes different from the quasi-synchronization mode $\Omega =$ (*1*) –2.5, (*2*) –5.3, and (*3*) –5.3; $F_0 =$ (*1*) 0.22, (*2*) 0.22, and (*3*) 0.32.

wave by analyzing the space-time dynamics of waves traveling along the interaction space.

At each point of the interaction space, one can introduce a frequency $\omega(\xi)$ defined according to formula (6) with the field phase at the system output $\xi = 0$ substituted with the value of φ_F at an arbitrary point ξ of interaction space.

Figure 4 demonstrates the calculated frequency of self-oscillations in the system as a function of coordinate ξ for various generation modes. Curve *A* shows function $\omega(\xi)$ calculated for the autonomous oscillation mode of the generator. One can see that the entire interaction space can be conventionally divided into two regions. In the first one, which is adjoined to the collector end of the system ($\xi \sim A$), the oscillation frequency varies continuously with decreasing coordinate ξ. At $\xi_c \approx 1.0$, the self-oscillation frequency of the system stabilizes. Consequently, the region $\xi \in (0, \xi_c)$ of the interaction space can be considered as the second region where oscillations have a single frequency equal to the generation frequency ω_0 of the system. In this case, one can conventionally speak of a certain transitional process developing along the interaction space of the system towards the tube's output end $\xi = A$ which takes place until the oscillation frequency $\omega(\xi) = \omega_0$ is established.

Let us now consider how the picture changes when the system is affected by the control signal at the point $\xi = A$. In the mode dissimilar to the quasi-synchronization mode, the space-time dynamics become complicated (see Fig. 4, curves *1–3*). One can distinguish three characteristic regions in the interaction space. In the first one, which is adjacent to the area $\xi = A$ (where the control signal is applied), oscillations occur at the frequency Ω of the external action. The length of this region can be considered as a certain synchronization length A_s. At a large phase nonlinearity of the system ($\sim\mu(1 - |\beta|^2)\beta$), the synchronization length depends strongly on the external signal parameters, in the first place, on the frequency Ω. As an example, one can compare curves *2* and *3* plotted at the same frequency Ω and different amplitudes $F_{03} > F_{02}$. One can see that the synchronization length is approximately the same in both cases. However, in curve *1* of Fig. 4, which was plotted at different detunings $\Omega - \omega_{0A}$, the synchronization length is considerably smaller.

With further progress towards the output end of the system, the synchronization mode is destroyed, and the self-oscillation frequency begins to depend strongly on the coordinate in the interaction space. This mode is similar to the oscillation mode of an autonomous system close to the collector end. With further progress along the interaction space, at a certain coordinate $\xi = \xi_c$, the mode characterize by the stabilization of self-oscillation frequency at the ω_0 level is established. However, in this mode, both generation frequency ω_0 and coordinate ξ_c depend strongly on the external control signal parameters.

In the quasi-synchronization mode, the self-oscillations are established at a single frequency equal to frequency Ω of the external signal in the entire interaction space (see Fig. 4, curve *S*).

Let us consider why the characteristic self-oscillation frequency changes along the system length. Figure 5 depicts the surfaces of space-time distributions of amplitude $|F(\xi, \tau)|$ and phase $\bar{\varphi}_F(\xi, \tau)$ of the field for the following oscillation modes: autonomous chaotic generation (Fig. 5a), absence of synchronization (Fig. 5b), and quasi-synchronization (Fig. 5c).

Figure 5a depicting the autonomous oscillations clearly shows that complicated dynamics of amplitude $|F|$, characterized by the appearance of multihump distributions $|F(\xi)|$, take place along the interaction space $\xi \in (\xi_c, A)$. As follows from works [11, 16, 17] analyzing the self-modulation modes in the long-interaction devices, such a situation can be related to the multiple phase rearrangement of oscillating electrons of the helical beam in the strong electric field, i.e., to the amplitude nonlinearity of the system. The phase rearrangement of the beam leads to the sharp jumps of the current ($I(\xi)$) and field ($F(\xi)$) phases. This, in turn, causes complicated and strongly irregular phase dynamics in the initial region $\xi > \xi_c$ (see Fig. 5a) of the propagation distance of the field wave. In this case, the characteristic frequency of field oscillations (see Fig. 4, curve *A*) determined in accordance with relationship (6) depends strongly on coordinate ξ. In the region close to the output end of the system ($\xi < \xi_c$), where the field amplitude has a large value and the beam's bunched current is

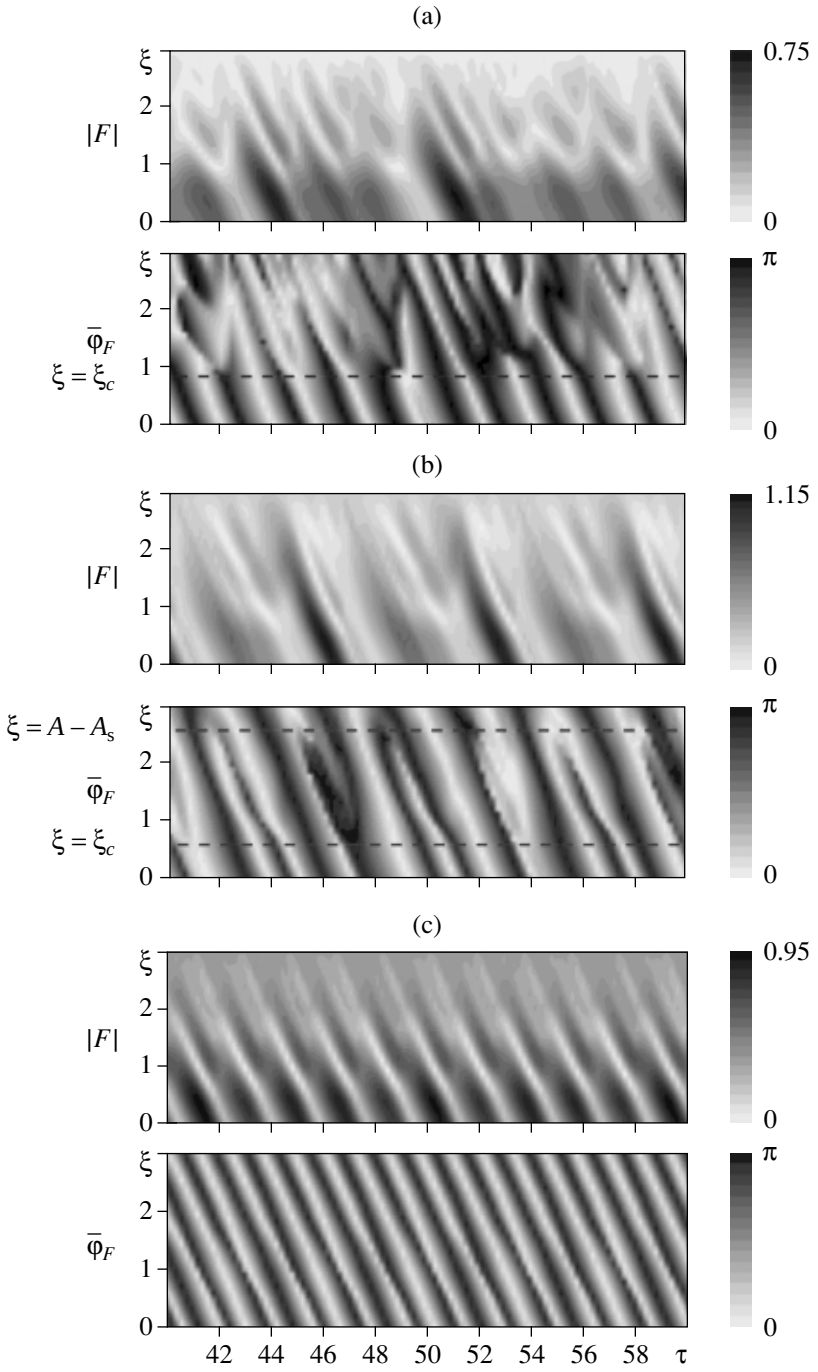

Fig. 5. Projections of the surfaces of space-time distributions of amplitude $|F|$ and phase φ_F of the field onto the (ξ, τ) plane for three oscillation modes: (a) autonomous generation in the system; (b) the mode different from the quasi-synchronization one which occurs at $\Omega = -2.5$ and $F_0 = 0.22$ (compare with curve *1* in Fig. 4); and (c) quasi-synchronization occurring at $\Omega = -5.3$ and $F_0 = 0.42$ (compare with curve *S* in Fig. 4).

small, the rearrangement of oscillating electrons is absent and the characteristic frequency of HF oscillations is stabilized. Coordinate ξ_c is determined by the length of the interaction space, in which the first harmonic of the bunched current reaches its maximum and the first electron structure (the phase bunch of oscillating electrons) is formed in the interaction space.

Let us now consider how the external signal affects the space-time dynamics of the system (see Fig. 5b corresponding to a mode dissimilar to the quasi-synchronization mode). One can see that, in the nonautonomous mode, the external signal causes the formation of a region $\xi \in (A - A_s, A)$ where the HF oscillations have the frequency Ω of external influence (Fig. 5b). In the

next large region of interaction space ($\xi \in (\xi_c, A - A_s)$), the destruction of the synchronization mode takes place, which is accompanied by sharp jumps and irregular dynamics of the field phase and, as a consequence, by the change in the bulk of the electron beam (the phase rearrangement of oscillating electrons of the helical beam). The destruction of the synchronization mode within the synchronization length A_s is determined by the violation of phase relationships $\Delta\varphi$ between the current and field waves, where the field phase advance $\Delta\varphi = |\Omega - \omega_0|A_s/v_g$ is determined by the influence of the control signal with frequency Ω. As a result, a complex structure of space-time distributions of field F and current I appears, which is related, as above, to the multiple phase rearrangement of the electron beam under the influence of a field with large amplitude. In the next region $\xi < \xi_c$, the characteristic frequency of HF oscillations is stabilized. Coordinate ξ_c now has another value as compared to the case of autonomous oscillations, because the process of the phase rearrangement of electron beam and, consequently, the maximization of the first harmonic of the bunched current are influenced by the frequency and amplitude of the external signal.

The quasi-synchronization mode (see Fig. 5c) is characterized by the regular dynamics of the field phase $\bar{\varphi}_F$ in the entire interaction space at the frequency Ω of external influence. The boundary of the quasi-synchronization region is determined by the condition that synchronization length A_s becomes equivalent to the length A of the interaction space. At $\mu = 8.0$ and $A = 3.0$, the system under study falls in the strongly nonlinear mode; therefore, frequency Ω_s corresponding to the boundary of the quasi-synchronization region is a complicated multiple-valued function of frequency Ω and amplitude F_0 of the external signal (see Section 3 and discussion of the formation of two quasi-synchronization regions).

Note that the self-modulation of the output signal is related to the appearance of an additional distributed feedback in the system [12, 18]. The helical electron beam bunched in the strong field reaches the collector end of the system ($\xi = A$) with velocity $v_\parallel$ after the rearrangement; the field excited by the beam moves towards the input end $\xi = 0$ of the system with velocity v_g, and the beam bunched in the weak field now excites a strong field in which the helical electron beam undergoes new rearrangement. As a result, the entire picture repeats itself with period $T \sim 2A(1/v_\parallel + 1/v_g)$, and time $T/2$ can be considered as a characteristic time delay in the appearance of an additional feedback circuit. As a result, the output signal becomes modulated with a characteristic time period $\sim T$.

CONCLUSION

The work analyzes the influence of an external harmonic signal on the chaotic self-oscillations in the simple model of CRM with a counterpropagating wave. It is shown that, within a certain range of control parameters, the phase synchronization (or quasi-synchronization) of the self-oscillations by the external signal entering the distributed active medium takes place. In the quasi-synchronization mode, generation of the output signal with slowly changing amplitude at the base frequency determined by the control signal is observed; the self-modulation of the output signal can be either periodic or chaotic. With considerable detuning of the external frequency from the frequency of autonomous generation and a large amplitude of the external influence, a complicated sequence of the order-to-chaos and chaos-to-order transitions takes place, depending on the frequency and amplitude of the control signal.

As far as the physical processes in the electron beam are concerned, the effect of an external control signal reduces to the influence on the internal distributed feedback formed in the helical-beam generator. The quasi-synchronization mode corresponds to the appearance of space-time oscillation modes at the frequency of external signal in the entire interaction space. The motion beyond the quasi-synchronization region occurring at the large value of nonisochronism parameter $\mu = 8.0$ is accompanied by the formation of three characteristic regions with different time oscillation frequencies. The mechanism of the self-modulation of the output signal is determined by the appearance of an additional distributed feedback and has the amplitude nature.

ACKNOWLEDGMENTS

This work was supported by the Russian Foundation for Basic Research, project nos. 00-15-96673 and 01-02-17392.

REFERENCES

1. Rulkov, N.F., Sushchik, M.M., Tsimring, L.S., and Abarbanel, H.D.I., *Phys. Rev. E*, 1995, vol. 51, no. 2, p. 980.
2. Pecora, L.M., Carroll, T.L., Jonson, G.A., and Mar, D.J., *Chaos*, 1997, vol. 7, no. 4, p. 520.
3. Afrimovich, V.S., Nekorkin, V.I., Osipov, G.V., and Shalfeev, V.D., *Ustoichivost', struktury i khaos v nelineinykh setyakh sinkhronizatsii* (Stability, Structures, and Chaos in the Nonlinear Synchronization Networks), Gaponov-Grekhov, A.V. and Rabinovich, M.I., Eds., Gor'kii: Inst. Prikl. Fiz. Akad. Nauk SSSR, 1989.
4. Rabinovich, M.I. and Trubetskov, D.I., *Vvedenie v teoriyu kolebanii i voln* (Introduction to the Oscillation and Wave Theory), Moscow–Izhevsk: NITs Regulyarn. Khaot. Din., 2000.
5. Rosenblum, M.G., Pikovsky, A.S., and Kurths, J., *Phys. Rev. Lett.*, 1996, vol. 76, no. 11, p. 1804.
6. Panter, P., *Modulation, Noise, and Spectral Analysis*, New York: McGraw-Hill, 1965.
7. Parlitz, U., Junge, L., and Lauterborn, W., *Phys. Rev. E*, 1996, vol. 54, no. 8, p. 2115.

8. Zhiganag Zheng and Gang Hu, *Phys. Rev. E*, 2000, vol. 62, no. 6, p. 7882.
9. Chu, K.R., Chen, H.Y., Hung, C.L., *et al.*, *Phys. Rev. Lett.*, 1998, vol. 81, no. 21, p. 4760.
10. Yulpatov, V.K., *Vopr. Radioelektron., Ser. 1: Elektron.*, 1965, no. 12, p. 15.
11. Kuznetsov, S.P. and Trubetskov, D.I., *Elektronika lamp s obratnoi volnoi* (Electronics of Backward-Wave Tubes), Saratov: Sarat. Gos. Univ., 1975, p. 135.
12. Dmitriev, A.Yu., Konevets, A.E., Pishchik, L.A., *et al.*, *Lektsii po elektronike SVCh i radiofizike: Materialy 7 zimnei shkoly-seminara inzhenerov* (Lectures on Microwave Electronics and Radiophysics: Proc. 7th Int. Winter School–Seminar of Engineers), Saratov: Sarat. Gos. Univ., 1986, p. 61.
13. Dmitriev, A.Yu., Trubetskov, D.I., and Chetverikov, A.P., *Izv. Vyssh. Uchebn. Zaved., Radiofiz.*, 1991, vol. 34, no. 9, p. 595.
14. Trubetskov, D.I. and Chetverikov, A.P., *Izv. Vyssh. Uchebn. Zaved., Prikl. Nelin. Din.*, 1994, vol. 2, no. 5, p. 3.
15. Khramov, A.E., *Radiotekh. Elektron.* (Moscow), 1999, vol. 44, no. 2, p. 211.
16. Ginzburg, N.S., Kuzntsov, S.P., and Fedoseeva, T.N., *Izv. Vyssh. Uchebn. Zaved., Radiofiz.*, 1978, vol. 21, no. 7, p. 1037.
17. Dmitrieva, T.V., Ryskin, N.M., Titov, V.N., and Shigaev, A.M., *Izv. Vyssh. Uchebn. Zaved., Prikl. Nelin. Din.*, 1999, vol. 7, no. 6, p. 66.
18. Kuznetsov, S.P., *Izv. Vyssh. Uchebn. Zaved., Radiofiz.*, 1982, vol. 25, p. 1410.